Extracting precise Higgs couplings by using the matrix element method

Jeppe R. Andersen, Christoph Englert, and Michael Spannowsky

Department of Physics, Institute for Particle Physics Phenomenology, Durham University, Durham DH1 3LE, United Kingdom
(Received 26 November 2012; published 14 January 2013)

After the recent discovery of a Standard Model Higgs bosonlike particle at the LHC, the question of its couplings to known and unknown matter is eminent. In this paper, we present a method that allows for an enhancement in signal over background (irreducible) of the order of 100% in $pp \to (h \to \gamma\gamma)jj$ for a center of mass energy of 8 and 14 TeV. This is achieved by applying the matrix element method. We discuss the implications of detector resolution effects and various approximations of the involved event simulation and reconstruction. The matrix element method provides a reliable, stable, and efficient handle to separate signal from background and the gluon and weak boson fusion components involved in this process. Employing this method, a more precise Higgs boson coupling extraction can be obtained, and our results are of immediate relevance for current searches.

I. INTRODUCTION

The performance of the CERN LHC and the rapid collection of data by both ATLAS and CMS will allow for detailed studies of the properties of the recently discovered boson [1,2] in the coming years. The first reported observations of the production cross section and branching fractions are consistent [3] with the expectation from a Standard Model Higgs boson [4] with the observed mass $m_h \simeq 126$ GeV, but sizeable uncertainties caused by the limited statistics are still present.

The projected amount of data collected this year will not only reduce these uncertainties but may also allow for the study of properties beyond total rates.

In many extensions of the Standard Model, the existence of $\mathcal{CP}$-odd bosons are predicted. Therefore, studying the $\mathcal{CP}$ properties of the boson is of great importance to confirm if the mechanism of electroweak symmetry breaking is minimal or not. A detailed study of the kinematic distributions in the production of the boson in association with two jets [5,6] will eventually allow for the direct measurement of the $\mathcal{CP}$ of the boson [7,8].

Equally important are direct measurements of the Higgs couplings to all other particles of the Standard Model. In particular, the loop-induced $h\gamma\gamma$ vertex is sensitive to new degrees of freedom, where direct production might be beyond the energy reach of the LHC. The number of observed signal events depends on the sum of the production processes and the decay branching ratio $h \to \gamma\gamma$. The branching ratio (BR), however, is inversely sensitive to all kinematically accessible final states in the Higgs decay, branching ratio $BR(\gamma\gamma) = \Gamma(h \to \gamma\gamma)/\Gamma(h \to \text{anything})$. Therefore, the precision in measuring any coupling of the Higgs boson obviously benefits from separating the production mechanisms because by forming ratios this dependence drops out.

In this respect, $pp \to hjj$ is important for two reasons. First we observe an excess in $h \to \gamma\gamma$ in current analyses,

especially in the $2j$ category [1,9]. Furthermore, an analysis of the $h \to \tau\tau$ channel heavily relies on the $2j$ final state. For $pp \to (h \to \tau\tau)jj$, we currently observe under production [2]. If both these findings prevail and follow from new physics beyond the SM, a precise investigation beyond simple ratios, which will also incorporate modifications of the gluon fusion (GF) and weak boson fusion (WBF) production modes, will majorly depend on WBF/ GF separation in this channel.

$pp \to (h \to \gamma\gamma)jj + X$ is roughly composed 50:50 by GF and WBF, depending on, e.g., the cut on the invariant dijet mass. In this context, it is important to note that the quantum interference between the GF and WBF components of $pp \to hjj + X$ production is completely negligible [10], and hence it is possible to consider these two contributions separately. Also, the theoretical uncertainty of the GF contribution is much larger than it is for WBF production [11,12], especially within the WBF selection cuts.

In this paper, we construct a likelihood function based on WBF and GF matrix elements that precisely serves this purpose to separate the production mechanisms, i.e., we apply the matrix element method [13] to the $pp \to (h \to \gamma\gamma)jj$ process on the fully showered and hadronized final state. We also generalize the GF vs WBF vs background discrimination in a realistic analysis by including the $pp \to \gamma\gamma + jj + X$ matrix elements. This constitutes the main irreducible background to this search [1]. Employing this strategy allows us to optimize cut scenarios to enhance signal over background (S/B). Given that the irreducible $pp \to \gamma\gamma jj$ constitutes $\mathcal{O}(70)\%$ of the total background [14], an additional handle to reduce it will greatly improve the sensitivity of the experimental analyses.

We organize this work as follows: First we discuss the matrix element strategy for $pp \to (h \to \gamma\gamma)jj + X$ for the LHC $\sqrt{s} = 14$ TeV in Sec. II. This is the setup for which most precision Higgs results can be obtained from a large

luminosity sample $\mathcal{L} \gtrsim 300$ fb^{-1}/experiment. We discuss the systematic uncertainties of various approximations of the signal event generation, especially for the GF contribution, and we also include the impact of finite detector resolution.

Equipped with these insights, we discuss the implications of the matrix element method for $pp \to (h \to \gamma\gamma)jj + X$ for the 8 TeV run and current results [1,2] in Sec. III. We conclude this work with a summary in Sec. IV.

II. HIGGS IN ASSOCIATION WITH TWO JETS AT 14 TeV

A. The matrix element method

Let us introduce the observables that we are going to study in the remainder of this paper. The GF/WBF discriminating likelihood is defined

$$
\begin{aligned}
&\tilde{Q}_n(p_1^\gamma, p_2^\gamma, \{p_n^j\}) \\
&= -\log\left[\frac{d\text{LIPS}(\gamma\gamma j^n)|\mathcal{M}^{\text{WBF}}(pp \to (h \to \gamma\gamma)j^n)|^2}{d\text{LIPS}(\gamma\gamma j^n)|\mathcal{M}^{\text{GF}}(pp \to (h \to \gamma\gamma)j^n)|^2}\right] \\
&= -\log\left[\frac{|\mathcal{M}^{\text{WBF}}(pp \to (h \to \gamma\gamma)j^n)|^2}{|\mathcal{M}^{\text{GF}}(pp \to (h \to \gamma\gamma)j^n)|^2}\right],
\end{aligned} \tag{2.1}
$$

where we denote the (partonic) jet multiplicity by n, dLIPS is the differential phase space weight for the particular kinematics (which is identical for all processes we consider and hence drops out of the ratio), and $|\mathcal{M}|^2$ denotes the respective matrix elements, already including the parton distribution functions (pdfs). We implement the CTEQ6L1 set [15] in the ratio of Eq. (2.1).

Equation (2.1) provides a one-dimensional probability distribution, which expresses statistical compatibility with either of the two hypotheses in the best suitable way, by definition. By including $\tilde{Q}_n$ to the event selection, we can optimize $\tilde{Q}_n \lesseqgtr \langle \tilde{Q}_n \rangle^{\text{WBF,GF}}$, depending on the purification requirement. The expectation values $\langle . \rangle$ follow from MC simulations of signal and background, similar to the construction of simple binned log-likelihood ratio hypothesis tests [16].

We apply the effective top approximation in the following for the GF contribution and the $h \to \gamma\gamma$ decay via operators [17]

$$
\mathcal{L} \supset \frac{\alpha_s}{12\pi v} G_{\mu\nu}^a G^{a\mu\nu} h + \frac{\alpha_{em}}{2\pi v} F_{\mu\nu} F^{\mu\nu} h(e_t^2 - 7/4). \tag{2.2}
$$

New degrees of freedom that alter the GF contribution and/or modify the Higgs couplings to weak bosons can be included as a global factor in the ratio of Eq. (2.1). A global factor merely shifts the $\tilde{Q}$ by a constant factor, which is irrelevant for the probabilistic discrimination of GF vs WBF. The model-specific details enter the sampling of $\langle \tilde{Q}_n \rangle^{\text{WBF,GF}}$ and in the individual normalizations.

The matrix elements that enter Eq. (2.1) are functions of parton-level kinematics, and we have to define an algorithm that maps the fully showered and hadronized jet final state to a suitable set of (massless) kinematics, which also includes information about the event's initial state. We do this in the following way: we first cluster jets with FASTJET [18] and reconstruct the isolated photons according to the respective analysis requirements (see further below). We count the number of jets passing the $p_{T,j}$ threshold in the events. We then redistribute the transverse recoil against unresolved radiation. We reconstruct the jets' momenta along the beam axis from massless calorimeter cell entries at a given pseudorapidity. We scale the energy of the resulting objects such that $p^2 = 0$. From the sum of these objects, we get an overall energy reconstructed boost of the considered particle system, which allows us to define two momentum fractions of initial state momenta. This way, starting from an exclusive number of reconstructed jets n_j and photons n_γ that comply with the analysis requirements, we end up with a set of parton-level four momenta, which we use for the calculation of the ratios $\tilde{Q}_n$. This procedure is obviously not limited to MC studies and can be incorporated by experiments straightforwardly.

To discriminate signal from background, we generalize Eq. (2.1) to the S/B, $S/\sqrt{B}$-improving likelihood

$$
\tilde{Q}_n^b(p_1^\gamma, p_2^\gamma, \{p_n^j\}) = -\log\left[\frac{\{|\mathcal{M}^{\text{WBF}}(pp \to (h \to \gamma\gamma)j^n)|^2 + |\mathcal{M}^{\text{GF}}(pp \to (h \to \gamma\gamma)j^n)|^2\}}{|\mathcal{M}^{2\gamma}(pp \to \gamma\gamma j^n)|^2}\right]. \tag{2.3}
$$

For the numerical implementation of Eqs. (2.1) and (2.2), we rely on a combination of MADGRAPH v4 [19] and VBFNLO [20].

B. Event generation and selection

We generate two- and three-jet CKKW-matched [21] and unmatched samples with SHERPA [22], which implements the effective top approximation in the gluon fusion channels [23]. The events are generated with SHERPA's

default CT10 [24] pdf set to avoid biasing the analysis of the likelihood distributions.

It is known that the effective theory does not provide a valid description of the phenomenology as soon as we are sensitive to momentum transfers larger than the top mass, e.g., $p_{T,j} \gtrsim m_t$. Cross sections, on the other hand, are reproduced at the percent level, which follows from smaller effective theory cross sections for $p_{T,h} \lesssim m_t$, cancelling the excess with respect to the full calculation for $p_{T,h} \gtrsim m_t$.

For large momentum transfers $p_{T,h} \sim 300$ GeV, the deviations become larger than $\mathcal{O}(30\%)$. To fully capture the dynamics in a two-dimensional likelihood, which extends Eqs. (2.1) and (2.3), by the inclusion of the event's energy scale, one would need to incorporate the full mass dependence and a parametrization of potential new physics.

To test our effective theory approximation (note that we both simulate and analyze the event within the effective approximation), we also analyze a GF event sample obtained with VBFNLO [20], which includes the full top and bottom contributions. We pass the parton-level events to HERWIG++ [25] for showering and hadronization. This allows us to asses the bias of analyzing the events with effective theory matrix elements.

Finite detector resolution effects give rise to an additional systematic uncertainty when we want to analyze the discriminating power of the matrix element method. To assess their impact on Eqs. (2.1) and (2.3), we model jet momentum uncertainties according to Ref. [26],

$$\frac{\Delta E}{E} = \frac{5.2}{E} \oplus \frac{0.16}{\sqrt{E}} \oplus 0.033. \qquad (2.4)$$

For the photons we have performed a comparison of the invariant diphoton mass against the experimental results of Refs. [1,2] and find that a resolution uncertainty parametrized by 3% describes the experimental situation sufficiently well for our purposes.

Details of the 14 TeV cut setup are currently unknown; they will depend on the new pileup and underlying event conditions as well as on the potential excess in the $pp \to (h \to \gamma\gamma)jj + X$ signal cross sections. For the remainder of this section, we therefore adopt a cut setup which is based on phenomenological analyses (see, e.g., Refs. [7,27,28]). In Sec. III we employ the current 8 TeV selection of ATLAS [1].

We reconstruct k_T jets [29] with cone size parameter $R = 0.8$ and threshold $p_{T,j} \geq 30$ GeV in the pseudorapidity range $|\eta_j| < 4.5$ and require $n_j \geq 2$. The exactly two isolated photons are required to be central in the electromagnetic calorimeter $|\eta_\gamma| < 2.5$ with $p_{T,\gamma} \geq 30$ GeV (we define a photon to be isolated if the electromagnetic and hadronic activity in the cone with size $R = 0.3$ is less then 10% of the E_T of the photon candidate, where R is again the distance in the azimuthal angle—pseudorapidity plane). The photons have to reconstruct the Higgs mass $m_h = 126$ GeV within 115^2 GeV$^2 \leq (p_{\gamma,1} + p_{\gamma,2})^2 \leq 135^2$ GeV^2. On top of these generic cuts, we impose a typical WBF selection: the two jets leading in p_T are required to have a large invariant mass $m_{j_1 j_2} \geq 600$ GeV and have to fall into opposite detector hemispheres $y_{j_1} \times y_{j_2} \leq 0$.

C. Performance of $\tilde{Q}_n$

For these 14 TeV selection criteria, we show the normalized distribution of the exclusive number of jets for
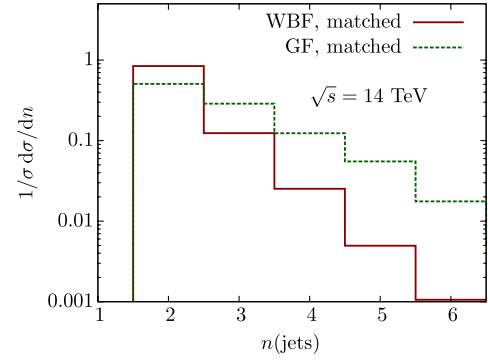

FIG. 1 (color online). Exclusive number of jets distribution for the LHC running 14 TeV. The selection cuts are described in the text.

14 TeV in Fig. 1 (for a detailed analysis of this observable see Ref. [30]). The cross sections are $\sigma^{GF} \simeq 0.61$ fb and $\sigma^{WBF} \simeq 1.58$ fb. From this we see that we can limit our analysis to $\tilde{Q}_n, \tilde{Q}_n^b$ for $n = 2, 3$. Higher jet multiplicities contribute at a level that is challenged by the theoretical uncertainties of the inclusive $p \to hjj + X$ cross sections [11,12]. The extension to $n > 3$ is technically straightforward.

We show our results in Fig. 2. An immediate first observation is that neither the definition of the likelihoods nor the impact of either detector resolution or details of the event simulation have a significant impact on the discriminating power of $\tilde{Q}_{n=2,3}$. Keeping in mind that we already look at WBF-like events and have a reconstructed Higgs boson, a cut on $\tilde{Q}_2$ will significantly enhance the WBF contribution over GF production. This is even more the case for $\tilde{Q}_3$. This can be understood along the following lines. Additional jet radiation in the WBF component[1] is essentially QCD bremsstrahlung off the leading jets, since there is no color exchange between the quark legs. This is entirely different for the GF contribution, which tends to populate the large available phase space in the central region with QCD activity [32]. Not only the presence of this radiation [33], but also, more importantly, the information that is encrypted in the differential energy-momentum flow associated with it [8] provides an elaborate handle to separate WBF from GF. This is most efficiently reflected in $\tilde{Q}_{n\geq3}$, of which only $n = 3$ is statistically relevant[2].

The result of GF/WBF purification is depicted in Fig. 3. Going to large values $|\tilde{Q}_{2,3}| \gg 1$, we recover a high level of purification within the limits of the selection criteria as expected, $\sigma^{GF}/\sigma^{WBF} \lesssim 0.1$, $\sigma^{GF}/\sigma^{WBF} \gtrsim 3$, respectively.

---

[1]For a detailed discussion of this contribution beyond LO see Ref. [31].

[2]The event shape observables discussed in Ref. [8] also capture sensitivity from relatively soft radiation which, by definition of $\tilde{Q}_n$ as jet- based observables, is not considered.
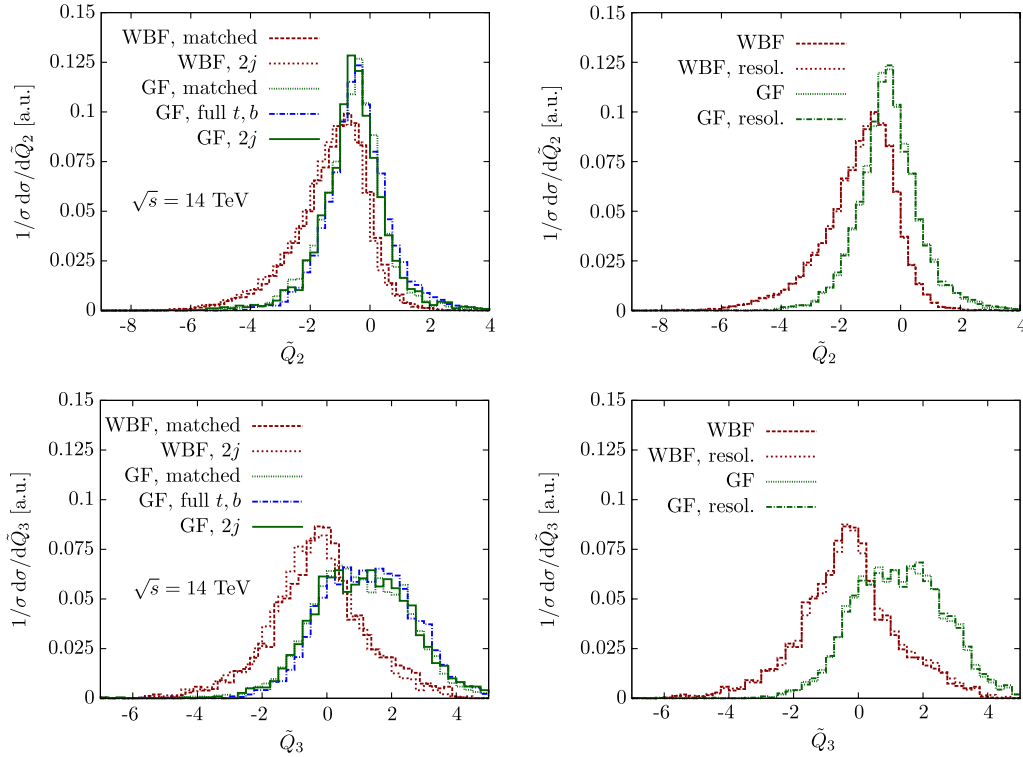
FIG. 2 (color online). Two-jet and three-jet likelihoods $\tilde{Q}_{2,3}$ for the cuts as described in the text and $\sqrt{s} = 14$ TeV. We show the influence of various event generation modes, where "$2j$" refers to generating $pp \to hjj \to \gamma\gamma jj$ events from two-jet matrix elementsm + parton shower, "matched" refers to a matched $2j/3j$ sample, and "full t, b" stands for two-jet events, including the full one-loop mass dependence, interfaced to the parton shower. We also show the influence of detector and photon resolution effects.

Comparing to Fig. 2, this comes at the price of increasingly small signal cross sections. A more realistic analysis (that also includes a more realistic description of the detector environment, pileup, etc.) needs to optimize the signal rate with respect to purification. Applying multiple cuts on $\tilde{Q}_n$ for an identically chosen basic cut setup, on the other hand, can be used to define distinct signal regions that allow us to reconstruct the WBF/GF content upon correlating the two measurements.

This finding needs to be contrasted to the standard paradigm of WBF/GF separation via a larger m_{jj} cut. In

Fig. 4, we show the relative fraction of full one-loop GF vs NLO QCD WBF for $\sqrt{s} = 14$ TeV as a function of the imposed m_{jj} selection. We see that the emerging quark-induced processes at large x for a stiff m_{jj} cut saturate the relative fraction at about 15%. The resulting event topology is WBF-like at small total cross sections. Central jet vetos can further decrease the relative contribution but challenge the perturbative description [6].

We now turn to signal vs background discrimination. In Fig. 5 we show the distributions for $\tilde{Q}_{2,3}^b$ for our $\sqrt{s} = 14$ TeV selection. Obviously, by cutting on $\tilde{Q}_{2,3}^b$, we can
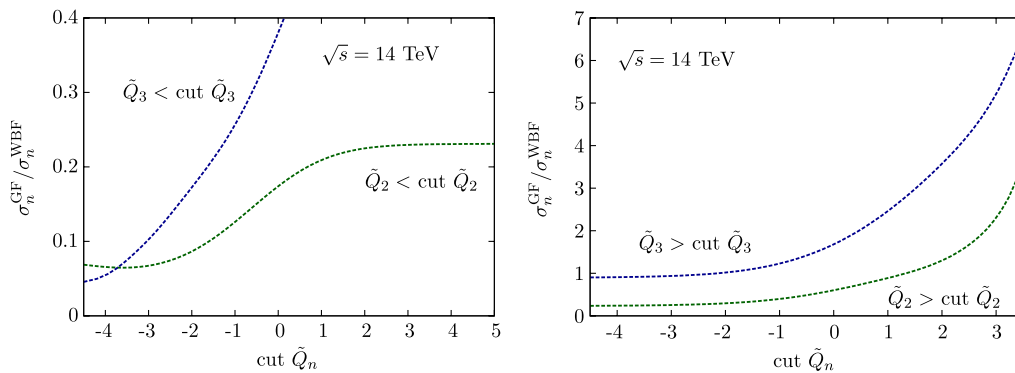

FIG. 3 (color online). Purification of GF vs WBF on the basis of the likelihood $\tilde{Q}_{2,3}$.
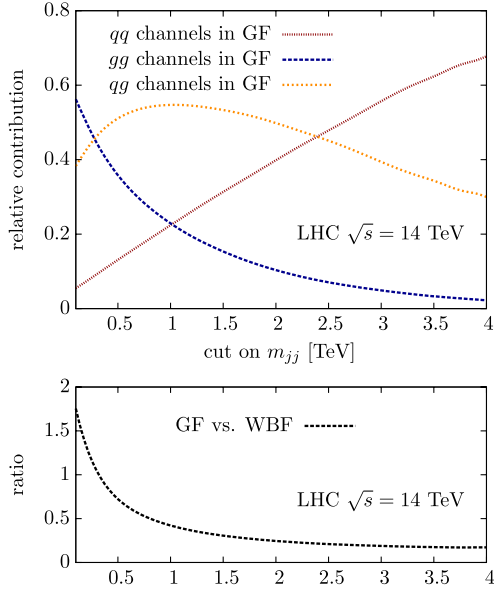
FIG. 4 (color online). $pp \to hjj$ production via gluon fusion (including full top and bottom contributions) broken down to the partonic channels and comparison of WBF (at NLO QCD) vs GF as a function of the cut on the invariant dijet mass. Results are obtained with VBFNLO [20].

purify the signal + background sample without too much signal loss. This way the signal compared to the irreducible background can be increased by >100%. It is worth noting that this will affect the GF and WBF contribution almost

identically (this is the reason why we choose to plot WBF and GF as separate samples in Fig. 5).

In order to gain a better handle on the GF distributions, we can relax the m_{jj} cut such that the event is not forced into a WBF-type topology. In Fig. 4, we also show distributions for $m_{jj} \geq 400$ GeV. As expected, the difference in the WBF/GF samples is now more pronounced in $\tilde{Q}_n^b$. The irreducible $\gamma\gamma$ background grows by approximately a factor of two while the gluon fusion and weak boson fusion cross sections are 0.95 and 2.1 fb. This is an increase by factors 1.6 and 1.3, respectively, compared to the $m_{jj} \geq$ 600 GeV selection. We find similar WBF/GF separation properties as in Fig. 3. Note that the irreducible background grows disproportionally, and a signal vs background enhancement will vitally depend on a good S/B discriminator, which is exactly provided by $\tilde{Q}_n^b$.

III. APPLICATION TO HIGGS IN ASSOCIATION WITH TWO JETS AT 8 TEV

We can straightforwardly adopt the strategy of Sec. II A to the current 8 TeV setup. The ATLAS selection for the two-jet category of the $h \to \gamma\gamma$ search is as follows [1]: we cluster anti-k_T jets [34] with FASTJET [18] for $R = 0.4$ and select at least two jets with $p_{T,j} \geq 25$ GeV and $p_{T,j} \geq 30$ in the more forward region $2.5 \leq |\eta_j| \leq 4.5$. The hardest jets are required to have a rapidity gap $|\Delta \eta_{jj}| \geq 2.8$ and the dijet system has to recoil against the diphoton system in
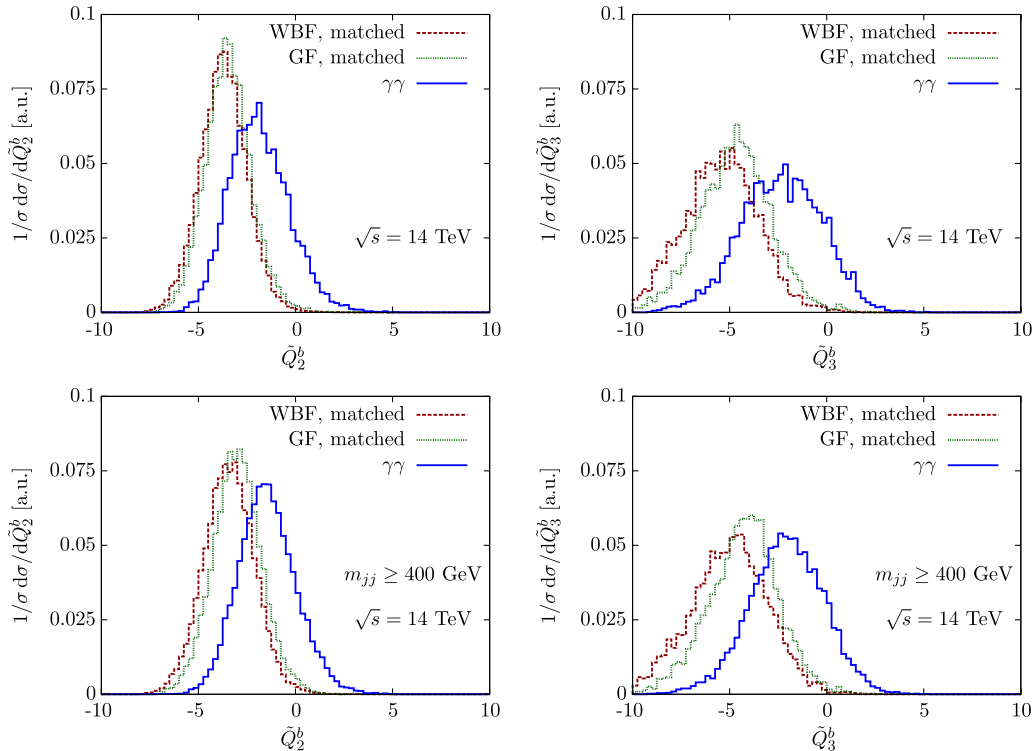

FIG. 5 (color online).   Two-jet and three-jet likelihoods $\tilde{Q}_{2,3}^b$ for the cuts as described in the text and $\sqrt{s} = 14$ TeV. Detector resolution effects are included. The lower panel gives results for a loosened cut set with $m_{jj} \geq 400$ GeV.
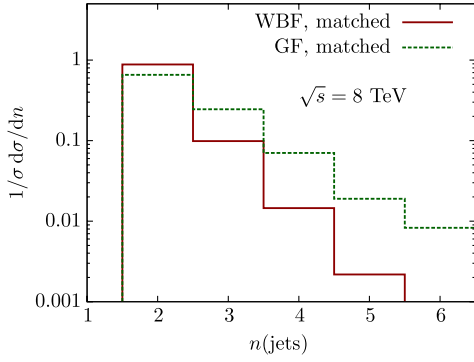
FIG. 6 (color online).   Exclusive number of jets distribution for LHC 8 TeV.

the transverse plane $\Delta\phi(jj, \gamma\gamma) \geq 2.6$. Again as in Sec. II we require a Higgs mass reconstruction within 20 GeV interval centered around $m_h = 126$ GeV.

The exclusive number of jets for this selection is again shown in Fig. 6; and we find agreement of our analysis with the experiment's quoted number of three expected events in 4.7 fb^{-1}. Obviously, there is again no need to go beyond $n = 3$.

Finally, we again analyze the potential S/B improvement (where B refers to the irreducible background for our purposes), which is the key limiting factor when dealing with the small event rates for the 8 TeV run. Figure 7 shows

a similar behavior as Fig. 5, and we infer that we can at least gain a factor of 100% in S/B without cutting into the signal count in the currently applied selection. All remarks of the 14 TeV results generalize to the lower energy of 8 TeV, and again the GF and WBF signals rates are affected identically by selecting events according to $\tilde{Q}^b_{2,3}$.

IV. SUMMARY AND CONCLUSIONS

In this paper, we have applied the matrix element method to $pp \rightarrow (h \rightarrow \gamma\gamma)jj$ production and investigated the prospects to separate the GF and WBF contributions. This is of utmost importance for $\mathcal{CP}$ analyses of the newly discovered particle, as well as for the measurement of its couplings to known matter. The same method can be applied to other decay modes of the Higgs boson, e.g., $h \rightarrow \tau\tau$.

We find that the matrix element method provides an excellent discriminator, which is stable against finite detector resolution effects and event generation systematics. We have extended WBF/GF separation to signal vs (irreducible) background discrimination and find promising results. WBF/GF separation and enhanced signal vs background discrimination can be achieved simultaneously. Our results are directly relevant for the current two-jet category of $h \rightarrow \gamma\gamma$ analysis, improving the sensitivity to the signal over the irreducible $\gamma\gamma$ background by $\gtrsim 100\%$, thus leading to a
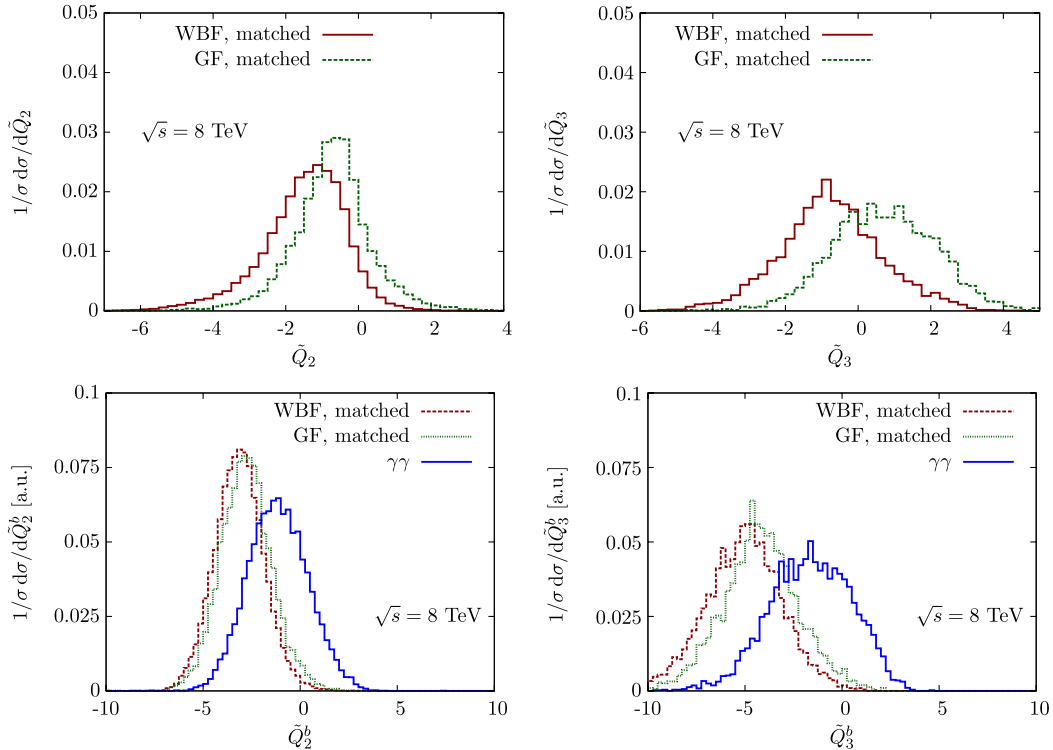

FIG. 7 (color online).   The matrix element observables $\tilde{Q}_2$, $\tilde{Q}_3$, $\tilde{Q}^b_2$ and $\tilde{Q}^b_3$ for 8 TeV, employing the Higgs search's two-jet category cuts of Ref. [1].

potential sensitivity increase by 35% when reducible backgrounds are considered unaltered.

Already in the presently available data sets using $\tilde{Q}_n^b$, the event selection cuts can be relaxed to boost the signal event count, and thus significance, without affecting S/B.

Selection strategies that are based on $\tilde{Q}_n^{(b)}$ in an experimentally realistic analysis will allow us to measure Higgs properties to better precision than currently foreseen. The implementation of the method will become publicly available to the experiments.

ACKNOWLEDGMENTS

[1] G. Aad *et al.* (ATLAS Collaboration), Phys. Lett. B **716**, 1 (2012).

[2] S. Chatrchyan *et al.* (CMS Collaboration), Phys. Lett. B **716**, 30 (2012).

[3] A. Azatov, R. Contino, and J. Galloway, J. High Energy Phys. 04 (2012) 127; D. Carmi, A. Falkowski, E. Kuflik, T. Volansky, and J. Zupan (unpublished); T. Corbett, O. J. P. Eboli, J. Gonzalez-Fraile and M. C. Gonzalez-Garcia, Phys. Rev. D **86**, 075013 (2012); P. P. Giardino, K. Kannike, M. Raidal, and A. Strumia, Phys. Lett. B **718**, 469 (2012); J. Ellis and T. You, J. High Energy Phys. 09 (2012) 123; J. R. Espinosa, C. Grojean, M. Muhlleitner, and M. Trott, arXiv:1207.1717; T. Plehn and M. Rauch, Europhys. Lett. **100**, 11002 (2012).

[4] F. Englert and R. Brout, Phys. Rev. Lett. **13**, 321 (1964); P. W. Higgs, Phys. Lett. **12**, 132 (1964); Phys. Rev. Lett. **13**, 508 (1964); G. S. Guralnik, C. R. Hagen, and T. W. B. Kibble, Phys. Rev. Lett. **13**, 585 (1964).

[5] G. Klamke and D. Zeppenfeld, J. High Energy Phys. 04 (2007) 052; J. R. Andersen and J. M. Smillie, J. High Energy Phys. 01 (2010) 039.

[6] J. R. Andersen, V. Del Duca and C. D. White, J. High Energy Phys. 02, (2009) 015.

[7] T. Plehn, D. L. Rainwater, and D. Zeppenfeld, Phys. Rev. Lett. **88**, 051801 (2002); K. Hagiwara, Q. Li, and K. Mawatari, J. High Energy Phys. 07 (2009) 101.

[8] C. Englert, M. Spannowsky, and M. Takeuchi, J. High Energy Phys. 06 (2012) 108.

[9] D. L. Rainwater and D. Zeppenfeld, J. High Energy Phys. 12 (1997) 005.

[10] J. R. Andersen, T. Binoth, G. Heinrich, and J. M. Smillie, J. High Energy Phys. 02 (2008) 057; A. Bredenstein, K. Hagiwara, and B. Jager, Phys. Rev. D **77**, 073004 (2008); L. J. Dixon and Y. Sofianatos, J. High Energy Phys. 08 (2009) 058.

[11] J. M. Campbell, R. K. Ellis, and G. Zanderighi, J. High Energy Phys. 10 (2006) 028.

[12] T. Figy, C. Oleari, and D. Zeppenfeld, Phys. Rev. D **68**, 073005 (2003); M. Ciccolini, A. Denner, and S. Dittmaier, Phys. Rev. Lett. **99**, 161803 (2007).

[13] K. Kondo, J. Phys. Soc. Jpn. **57**, 4126 (1988); K. Kondo, J. Phys. Soc. Jpn. **60**, 836 (1991); V. M. Abazov *et al.* (D0 Collaboration), Nature (London) **429**, 638 (2004); K. Cranmer and T. Plehn, Eur. Phys. J. C **51**, 415 (2007); F. Fiedler, A. Grohsjean, P. Haefner, and P. Schieferdecker, Nucl. Instrum. Methods Phys. Res., Sect. A **624**, 203 (2010); P. Artoisenet, V. Lemaitre, F. Maltoni, and O. Mattelaer, J. High Energy Phys. 12 (2010) 068; J. Alwall, A. Freitas, and O. Mattelaer, Phys. Rev. D **83**, 074010 (2011); D. E. Soper and M. Spannowsky, Phys. Rev. D **84**, 074002 (2011); J. M. Campbell, W. T. Giele, and C. Williams, arXiv:1205.3434; P. Avery, D. Bourilkov, M. Chen, T. Cheng, A. Drozdetskiy, J. S. Gainer, A. Korytov, and K. T. Matchev *et al.*, arXiv:1210.0896.

[14] G. Aad *et al.* (ATLAS Collaboration), arXiv:1211.1913.

[15] J. Pumplin, D. R. Stump, J. Huston, H. L. Lai, P. M. Nadolsky, and W. K. Tung, J. High Energy Phys. 07 (2002) 012.

[16] T. Junk, Nucl. Instrum. Methods Phys. Res., Sect. A **434**, 435 (1999); T. Junk, CDF Note 8128 (http://cdf/doc/statistics/public/8128); T. Junk, CDF Note 7904 (http://cdf/doc/statistics/public/7904); H. Hu and J. Nielsen, in 1st Workshop on Confidence Limits, CERN Report No. 2000-005 (2000).

[17] B. A. Kniehl and M. Spira, Z. Phys. C **69**, 77 (1995).

[18] M. Cacciari, G. P. Salam, and G. Soyez, Eur. Phys. J. C **72**, 1896 (2012).

[19] J. Alwall, P. Demin, S. de Visscher, R. Frederix, M. Herquet, F. Maltoni, T. Plehn, D. L. Rainwater, and T. Stelzer, J. High Energy Phys. 09 (2007) 028.

[20] K. Arnold, M. Bahr, G. Bozzi, F. Campanario, C. Englert, T. Figy, N. Greiner and C. Hackstein *et al.*, Comput. Phys. Commun. **180**, 1661 (2009).

[21] S. Catani, F. Krauss, R. Kuhn, and B. R. Webber, J. High Energy Phys. 11 (2001) 063.

[22] T. Gleisberg, S. Hoeche, F. Krauss, M. Schonherr, S. Schumann, F. Siegert, and J. Winter, J. High Energy Phys. 02 (2009) 007; S. Schumann and F. Krauss, J. High Energy Phys. 03 (2008) 038; T. Gleisberg and S. Hoeche, J. High Energy Phys. 12 (2008) 039; S. Hoeche, F. Krauss, S. Schumann, and F. Siegert, J. High Energy Phys. 05 (2009) 053.

[23] F. Krauss, R. Kuhn, and G. Soff, J. High Energy Phys. 02 (2002) 044.

[24] H.-L. Lai, M. Guzzi, J. Huston, Z. Li, P. M. Nadolsky, J. Pumplin and C.-P. Yuan, Phys. Rev. D **82**, 074024 (2010).

[25] M. Bahr, S. Gieseke, M. A. Gigg, D. Grellscheid, K. Hamilton, O. Latunde-Dada, S. Platzer and P. Richardson *et al.*, Eur. Phys. J. C **58**, 639 (2008).

[26] G. Aad *et al.* (ATLAS Collaboration), JINST **3**, P07007 (2008); G. L. Bayatian *et al.* (CMS Collaboration), J. Phys. G **34**, 995 (2007).

[27] V. Del Duca, W. Kilgore, C. Oleari, C. R. Schmidt, and D. Zeppenfeld, Phys. Rev. D **67**, 073003 (2003); F. Campanario, M. Kubocz, and D. Zeppenfeld, Phys. Rev. D **84**, 095025 (2011).

[28] V. Hankele, G. Klamke, D. Zeppenfeld, and T. Figy, Phys. Rev. D **74**, 095001 (2006).

[29] S. Catani, Y. L. Dokshitzer, M. H. Seymour, and B. R. Webber, Nucl. Phys. **B406**, 187 (1993); S. D. Ellis and D. E. Soper, Phys. Rev. D **48**, 3160 (1993).

[30] E. Gerwick, T. Plehn, and S. Schumann, Phys. Rev. Lett. **108**, 032003 (2012).

[31] T. Figy, V. Hankele, and D. Zeppenfeld, J. High Energy Phys. 02 (2008) 076.

[32] Y. L. Dokshitzer, V. A. Khoze, and T. Sjostrand, Phys. Lett. B **274**, 116 (1992).

[33] B. E. Cox, J. R. Forshaw, and A. D. Pilkington, Phys. Lett. B **696**, 87 (2011).

[34] M. Cacciari, G. P. Salam, and G. Soyez, J. High Energy Phys. 04 (2008) 063.